Intrinsically disordered linkers control tethered kinases via effective concentration

Mateusz Dyla[a,b] and Magnus Kjaergaard[a,b,c,d,1]

[a]Department of Molecular Biology and Genetics, Aarhus University, DK-8000 Aarhus, Denmark; [b]Danish Research Institute of Translational Neuroscience - DANDRITE, Nordic-EMBL (European Molecular Biology Laboratory) Partnership for Molecular Medicine, DK-8000 Aarhus, Denmark; [c]Center for Proteins in Memory, Danish National Research Foundation, DK-8000 Aarhus, Denmark; and [d]Aarhus Institute of Advanced Studies, Aarhus University, DK-8000 Aarhus, Denmark

Edited by William F. DeGrado, University of California, San Francisco, CA, and approved July 27, 2020 (received for review April 5, 2020)

Kinase specificity is crucial to the fidelity of signaling pathways, yet many pathways use the same kinases to achieve widely different effects. Specificity arises in part from the enzymatic domain but also from the physical tethering of kinases to their substrates. Such tethering can occur via protein interaction domains in the kinase or via anchoring and scaffolding proteins and can drastically increase the kinetics of phosphorylation. However, we do not know how such intracomplex reactions depend on the link between enzyme and substrate. Here we show that the kinetics of tethered kinases follow a Michaelis–Menten-like dependence on effective concentration. We find that phosphorylation kinetics scale with the length of the intrinsically disordered linkers that join the enzyme and substrate but that the scaling differs between substrates. Steady-state kinetics can only partially predict rates of tethered reactions as product release may obscure the rate of phosphotransfer. Our results suggest that changes in signaling complex architecture not only enhance the rates of phosphorylation reactions but may also alter the relative substrate usage. This suggests a mechanism for how scaffolding proteins can allosterically modify the output from a signaling pathway.

intrinsically disordered protein | kinase | effective concentration | signaling complex | scaffolding protein

Cellular signaling relies on cascades of enzymes such as protein kinases and phosphatases. Signaling fidelity requires kinases to use specific substrates, although the same kinases can take part in different pathways with different substrates. For example, protein kinase A (PKA) is involved in signaling pathways throughout cell biology (1). Kinase specificity arises in part from the linear motifs surrounding the phospho-accepting residue. However, in vivo substrate usage can only be predicted partially from sequences motifs as kinase signaling is also regulated through the local abundance of enzymes (2). The latter class of effects is much less understood quantitatively.

The local abundance of signaling enzymes is regulated at many levels. At the cellular level, kinases are targeted to, e.g., an organelle or the cell membrane. At the molecular level, enzymes are targeted to a subset of their potential substrates by tethering to scaffolding proteins. In multidomain enzymes, such tethering occurs via protein interaction domains attached to the catalytic domain (3). Alternatively, enzymes can be tethered by scaffolding proteins that bind the enzyme and substrates noncovalently (4). PKA is regulated by more than 50 different A kinase anchoring proteins (AKAPs) that direct the kinase to different pathways (5). PKA may dissociate from its regulatory subunit and thus AKAPs upon activation, but recently, it was demonstrated that active PKA may remain tethered to AKAP (6). The intrinsically disordered AKAPs thus restrict the kinase to a region whose dimensions are defined by the length and compactness of the anchoring protein (7). Similarly, disordered linkers of variable length regulate the activity of the dodecameric kinase CaMKII by controlling the balance between intersubunit and intrasubunit phosphorylation (8). Many kinase signaling reactions thus occur internally in proteins or in protein complexes.

When a kinase is physically associated to its substrate, the tethered substrate is distinct from all other substrates in the reaction mixture and is usually phosphorylated much faster. The kinetics of such reactions differ from steady-state enzyme kinetics as tethered catalysis is effectively single turnover. Due to the switch-like functions of many kinases, they may only need to phosphorylate a single substrate to exert a biological function (9). This can be seen, e.g., in the negative feedback loop formed by AKAP79-tethered PKA, which inactivates adenylate cyclase by phosphorylation (10). The rate of intramolecular (or intracomplex) reactions is expected to be concentration independent, although this is rarely tested for tethered kinases. Instead, the encounter rate is determined by the connection between enzyme and substrate. The quantitative description of tethered catalysis is hindered by the lack of framework to describe the connection in kinetic terms. We propose that many linkers can be accounted for by the effective concentration of substrate they enforce. Enzyme scaffolding proteins and interdomain linkers in kinases are often intrinsically disordered as they allow the kinase domain to search for its substrates (11). For fully disordered linkers, the effective concentrations can be estimated from power law scaling with the length of the linker (12). Kinases tethered by disordered protein linkers thus offer a chance to understand the general principles that govern tethered catalysis.

Here we investigate how the connection between a kinase and its substrate affects the phosphorylation kinetics. We use a model system consisting of the catalytic domain of PKA tethered to a

Significance

Kinases are often tethered to their substrates, and many phosphorylation reactions thus occur inside macromolecular complexes. However, it is currently not known how such tethering affects the rate of phosphorylation. We show that tethering can enhance the rate by orders of magnitude but that the enhancement is highly sensitive to the length of the linker. We provide an equation describing tethered reactions and show that their rates can only partially be predicted from untethered reactions. We suggest a mechanism for how changes in linkers and scaffolding proteins may alter the output of signaling pathways.

Author contributions: M.D. and M.K. designed research; M.D. performed research; M.D. contributed new reagents/analytic tools; M.D. and M.K. analyzed data; and M.D. and M.K. wrote the paper.

The authors declare no competing interest.

This article is a PNAS Direct Submission.

Published under the PNAS license.

[1]To whom correspondence may be addressed. Email: magnus@mbg.au.dk.

This article contains supporting information online at https://www.pnas.org/lookup/suppl/doi:10.1073/pnas.2006382117/-/DCSupplemental.

First published August 18, 2020.

substrate via variable intrinsically disordered linkers. We show that phosphorylation rate varies by several orders of magnitude depending on the substrate and the linker. We show that phosphorylation rate follows a Michaelis–Menten like dependence on the effective concentration enforced by the linker, with steady-state parameters partially predicting the rates of tethered single turnover phosphorylation. This provides a baseline for interpreting how signaling complex architecture regulates tethered enzymes.

Materials and Methods

Preparation of DNA Constructs. The plasmid containing the catalytic domain of PKA (PKAc) was a gift from Susan Taylor (Department of Chemistry and Biochemistry and Pharmacology, University of California San Diego, La Jolla, CA) via Addgene (no. 14921) (13). The other plasmids were prepared by de novo synthesis by Genscript and codon optimized for expression in *Escherichia coli*. The coding regions were cloned into pET15b vectors using the NdeI/XhoI sites. The disordered GS linkers from the linker library generated previously (12) were cloned into the protein constructs using unique NheI/KpnI sites. The sequences of protein constructs are given in *SI Appendix*.

Protein Expression and Purification. Protein constructs containing the catalytic domain of PKA linked by variable length linkers to the MBD2 coiled-coil domain [MBD2-$(GS)_n$-PKAc] were expressed in C41(DE3) cells in LB medium with 100 μg/mL ampicillin at 37 °C and shaking at 120 rpm. The cultures were induced with 1 mM IPTG at OD_{600} = 0.6 to 0.8, and the temperature was decreased to 30 °C for an overnight expression. Protein constructs containing PKA substrates linked to the p66α coiled-coil domain [p66α-$(GS)_n$-substrate] were expressed in BL21(DE3) cells in ZYM-5052 autoinduction medium (14) containing 100 μg/mL ampicillin at 37 °C and shaking at 120 rpm overnight.

The cells were harvested by centrifugation (15 min, 6,000 × *g*), and bacterial pellets were resuspended in binding buffer (20 mM NaH_2PO_4, 0.5 M NaCl, 5 mM imidazole, 0.1 mM TCEP, 0.2 mM PMSF, 50 mg/L of leupeptin, 50 mg/L pepstatin, 50 mg/L chymostatin, pH 7.4) and lysed by sonication (50% duty cycle, maximum power of 75%, sonication time of 6 min). The lysate was centrifuged (20 min, 27,000 × *g*) and the supernatant was applied to gravity flow columns packed with Ni-NTA Superflow (QIAGEN). The columns were washed with buffers containing increasing concentrations of imidazole (20 to 50 mM) and were eluted with elution buffer (20 mM NaH_2PO_4, 0.5 M NaCl, 500 mM imidazole, 0.1 mM TCEP). Eluted protein samples containing PKA substrates were dialyzed against binding buffer without imidazole overnight, followed by cleavage of His-tag by thrombin (1:1,000 thrombin to substrate ratio) at 37 °C and shaking at 300 rpm for 30 min. Cleaved samples were applied to gravity flow columns packed with Ni-NTA Superflow (QIAGEN), and flow-through was collected. All protein samples were additionally purified by size-exclusion chromatography (SEC) in TBS buffer (20 mM Tris-base, 150 mM NaCl, 0.1 mM TCEP, pH 7.6) using Superdex 200 Increase and Superdex 75 Increase columns (GE Healthcare) to purify PKAc and its substrates, respectively.

Quench–Flow Measurements. Single-turnover kinetic measurements were performed using a KinTek Corporation RQF-3 Rapid quench–flow instrument at 30 °C. MBD2-$(GS)_n$-PKAc and p66α-$(GS)_n$-substrate were diluted to 10× final concentration in enzyme dilution buffer (50 mM Tris-base, 0.1 mM EGTA, 1 mg/mL BSA, 1 mM TCEP, pH 7.6) and TBS (20 mM Tris-base, 150 mM NaCl, pH 7.6), respectively. Quench–flow experiments were executed by loading the catalytic domain of PKA and its substrates (final concentration 0.5 μM unless indicated otherwise) into one sample loop and [γ-^{32}P]ATP (final concentration 0.1 mM of 100 to 200 cpm pmol^{-1}) into the other. Phosphorylation reactions were carried out in the reaction buffer composed of 50 mM Tris-base, 0.1 mM EGTA, 10 mM magnesium acetate, 150 mM NaCl, pH 7.6. The reactions were quenched using 150 mM phosphoric acid using the constant quench option to limit the total quenched reaction volume to 70 μL. Phosphorylated substrates were separated from unreacted ATP by spotting the quenched reactions onto P81 phosphocellulose disks (Jon Oakhill, St. Vincent Institute, Melbourne, VIC, Australia). The filters were washed three times with 75 mM phosphoric acid, rinsed with acetone, dried, and counted on the ^{32}P channel in scintillation counter as cpm. Control experiments were performed to determine background phosphorylation level of substrate motifs in the absence of PKAc, as well as autophosphorylation of PKAc in the absence of substrates. Background values (typically negligible) were subtracted from the raw data. Specific phosphorylation was determined as amount of ^{32}P-incorporated substrate (pmol) based on [^{32}P]ATP standard curve, where cpm values of known amounts of spiked [^{32}P]ATP were measured.

Steady-State Kinetics. PKAc (without the MBD2 dimerization domain) was diluted to 10× final concentration in enzyme dilution buffer (50 mM Tris-base, 0.1 mM EGTA, 1 mg/mL BSA, 1 mM TCEP, pH 7.6), and p66α-$(GS)_n$-substrate was diluted to 5× final concentration in TBS (20 mM Tris-base, 150 mM NaCl, pH 7.6). Steady-state experiments were executed by manual addition of [γ-^{32}P]ATP (final concentration 0.1 mM of 100 to 200 cpm pmol^{-1}) into reaction mix containing 1 nM PKAc and p66α-$(GS)_n$-substrate (final concentration 10 to 1,820 μM) in a reaction buffer (50 mM Tris-base, 0.1 mM EGTA, 10 mM magnesium acetate, 150 mM NaCl, pH 7.6) at 30 °C. Every minute, 5 μL of the reaction mix was spotted onto a P81 filter disk and placed into 75 mM phosphoric acid to quench the reaction. The filters were washed three times with 75 mM phosphoric acid, rinsed with acetone, dried, and counted on the ^{32}P channel in scintillation counter as cpm. Control experiments were performed in the same way as in quench–flow experiments, and specific phosphorylation was determined likewise. Initial velocities at different substrate concentrations were derived from a slope of a linear regression as pmol of ^{32}P-incorporated substrate per minute. The data were then fitted by a Michaelis–Menten model, and k_{cat} was calculated by diving V_{max} by 0.005 pmol of PKAc and by 60 (min/s).

Results

To probe the linker dependence of tethered catalysis, we designed a model system composed of the catalytic domain of protein kinase A (PKAc) tethered to its substrate via disordered linkers (Fig. 1*A* and *SI Appendix*, Fig. S1). We used the optimal PKA substrate (WT in the following) and varied substrate quality by mutagenesis. PKA recognizes positive residues in positions −2 and −3 relative to the phosphorylation site with a preference for arginine over lysine (15). To weaken the site, we mutated each of the two arginine residues in the substrate motif to lysine resulting in variants R-2K and R-3K. The kinase and substrate were made as separate proteins and joined noncovalently using heterodimeric coiled-coil domains. We use the antiparallel coiled-coil formed between p66α and MBD2 (16) as it has low nanomolar affinity and is stable on the timescale of the tethered reaction. The coiled-coil domains were joined to the PKAc/substrate by an exchangeable linker flanked by restriction sites compatible with our library of disordered linkers (12). To approximate passive, entropic spacers, we used either a glutamate and a serine, or glycine–serine repeat linkers containing 20, 60, and 120 residues.

We followed single-turnover phosphorylation in an equimolar mix of kinase and substrate using quench–flow. The reaction was started by adding [γ-^{32}P]ATP, quenched by phosphoric acid at reaction times from 2.5 ms to 330 s, and followed from the amount of ^{32}P in the substrate. Initially, we compared identical tethered and untethered reactions, where tethering increased reaction rate by more than 100-fold (Fig. 1*B*). Intracomplex reactions are concentration independent, whereas the rate of bimolecular reactions increases with concentration. Therefore, we tested how the concentration of the enzyme and substrate affected the phosphorylation rate. While remaining below the K_M of the substrate, the concentration was increased 10-fold, which led to a slightly slower phosphorylation (Fig. 1*C*). These observations suggest that phosphorylation occurs intracomplex with negligible contributions from transphosphorylation.

To test how linkers affect phosphorylation, we varied the lengths of the GS repeats. By combining kinase and substrate variants, we created six complexes with a combined linker length spanning from 20 to 180 disordered residues in addition to the 17 residues from restriction sites and the short extra linker in the substrate. For all variants the phosphorylation reaction could be described well with a single exponential model (*SI Appendix*, Fig. S2), where the phosphorylation rate decreased monotonically with increased linker length (Fig. 2*A* and *SI Appendix*, Fig. S3). This suggests that kinase linkers and anchoring proteins directly regulate intracomplex kinase reactions.

Next, we tested whether substrate quality affects the linker dependence of phosphorylation. The phosphorylation rate decreased monotonically with linker length for the WT and both

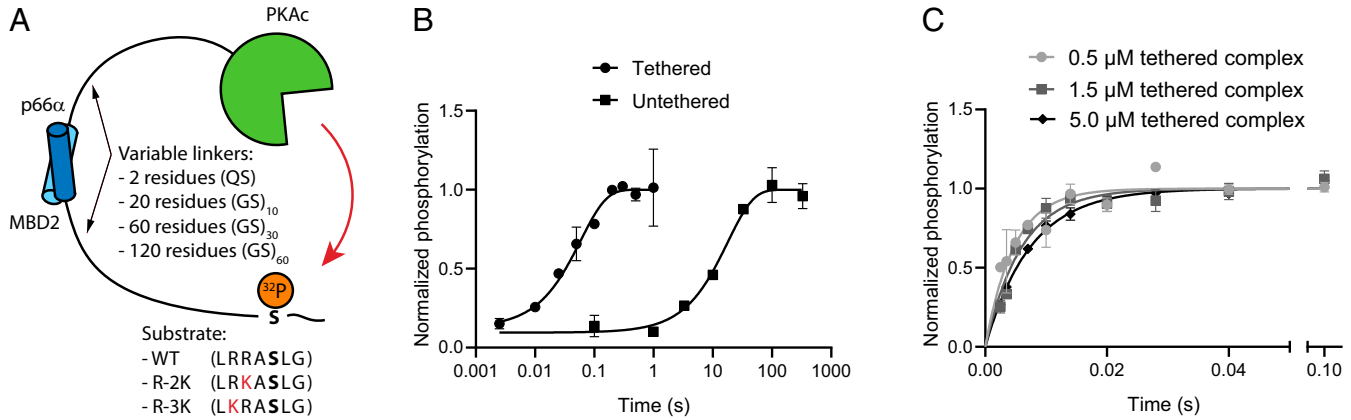

Fig. 1. A reductionist model system for tethered phosphorylation. (*A*) The catalytic domain of PKA and its consensus substrate motif are joined to the coiled-coil domain from MBD2 and p66α, respectively. MBD2 and p66α form an antiparallel heterodimer with nanomolar affinity (16). Substrate quality was varied by mutation away from the consensus motif, and the linker was varied by including GS repeats of variable length. Amino acid sequence of all substrates is shown, with the mutated residues marked in red and phosphorylated serine shown in bold. (*B*) Quench–flow was used to measure single-turnover kinetics by following incorporation of ^{32}P into the substrate. Tethering of enzyme [MBD2-$(GS)_{10}$-PKAc] to substrate [p66α-$(GS)_{10}$-R-2K, combined linker length of 40 residues] increased the rate by ∼300-fold at a substrate and enzyme concentrations of 0.5 μM. (*C*) The rate of the tethered catalysis decreased slightly with increasing concentration of the tethered complex [MBD2-$(GS)_{30}$-PKAc and p66α-$(GS)_{30}$-WT]. Error bars indicate mean ± SD, $n = 2$.

mutants, although with different magnitudes (Fig. 2*B*). Phosphorylation of the WT substrate only slows twofold from the shortest to the longest linkers, whereas the R-3K substrate slows by more than 10-fold. This suggests that substrates are affected differently by tethering and that the properties of the linker and substrate should be considered together.

The attenuated linker dependence of the WT substrate could in principle be caused by ATP binding becoming the limiting factor at high phosphorylation rates. To test this possibility, we carried out quench–flow experiments at a 1 mM ATP instead of 100 μM. The amount of [γ-^{32}P]ATP was kept constant to stay within permitted radioactivity levels, and so we increased the protein concentration to 5 μM, which had a minimal effect on kinetics (Fig. 1*C*), to maintain a robust signal. For the WT substrate, phosphorylation rates increased by ∼30% (*SI Appendix*, Fig. S4) for all linker combinations. A uniform rate enhancement at 1 mM ATP is expected if the kinase is not fully saturated with ATP at 100 μM. Previous studies report a K_M for ATP of 10 μM at different buffer conditions (17), so the kinase may not be fully saturated at 100 μM. To test this explanation, we also tested a slower R-3K variant with 1 mM ATP and saw a similar increase in the observed rate (*SI Appendix*, Fig. S2) consistent with an increase in level of bound ATP. This suggests that the attenuated linker dependence for the WT is not due to ATP binding becoming kinetically limiting but rather represents saturation of the tethered substrate.

Tethered reactions are expected to follow first-order kinetics with the contact frequency of reactants determined by their physical connection (18). The contact frequency can be expressed as an effective concentration, which in our case corresponds to the concentration of free substrate that would encounter the enzyme as often as the tethered substrate. Such effective concentration can occasionally be measured by competition experiments (12, 19, 20), although in most proteins has to be estimated theoretically (21–23). Our group previously measured the scaling of effective concentrations with the length of disordered linkers including the sequences used here (12). To estimate the effective concentration of the tethered substrate, we used the power law determined for GS-linkers previously and plotted phosphorylation rates as a function of effective concentration (Fig. 2 *C*–*E*). The tether in our kinase–substrate system also includes the coiled-coil domain, which acts as a rigid link in the flexible linker. Previous effective concentration measurements suggest a similar scaling with linker length for such a system, so we disregard the contribution of the coiled-coil domain although it potentially introduces a systematic error (19).

The phosphorylation rate saturated at high effective concentration for all variants. The WT substrate was close to saturation already at the concentrations enforced by the longest linkers. In contrast, R-2K only saturated at the highest effective concentration enforced by the shortest linkers, whereas R-3K had not plateaued yet at the highest effective concentration. The maximal rate also differed strongly between the substrates, as the R-2K and R-3K variants saturated at much lower rates than the WT substrate. In total, this suggests that the single turnover reaction can be described by a Michaelis–Menten-like dependence on the effective concentration with a halfway saturation point and maximal turnover characteristic of each substrate, where $k_{tet,max}$ is the maximum phosphorylation rate and $C_{eff,50}$ is an effective concentration at half-saturation:

$$k_{tet} = \frac{k_{tet,max} C_{eff}}{C_{eff,50} + C_{eff}}. \quad [1]$$

To describe the kinetics of tethered phosphorylation reactions, we derived rate equations (*SI Appendix*, text) based on a product-release limiting model for PKA (Fig. 3) (17, 24). The model is simplified by assuming stable tethering of the kinase to its substrate. This is approximated well by high-affinity anchoring interactions as in our model system, where the anchoring interaction has nanomolar affinity and half-life of minutes (16). Under the assumption that phosphorylation (k_2) and product release (k_3) are irreversible and the closed, catalytically competent complex (C) is in a rapid equilibrium with an open form (O), the rate of phosphorylation in the tethered system (k_{tet}) follows the following relationship on effective concentration (C_{eff}):

$$k_{tet} = \frac{k_2 C_{eff}}{K_d + C_{eff}}. \quad [2]$$

The rate of phosphotransfer (k_2) is directly obtained from the maximum rate of phosphorylation in the tethered system ($k_{tet,max}$), and K_d is obtained from an effective concentration at half-saturation $C_{eff,50}$, based on the fit of experimental data to Eq. 1. The fitting parameters are given in Table 1. K_d determined in this way for the WT substrate is equal to 142 μM, similar to the

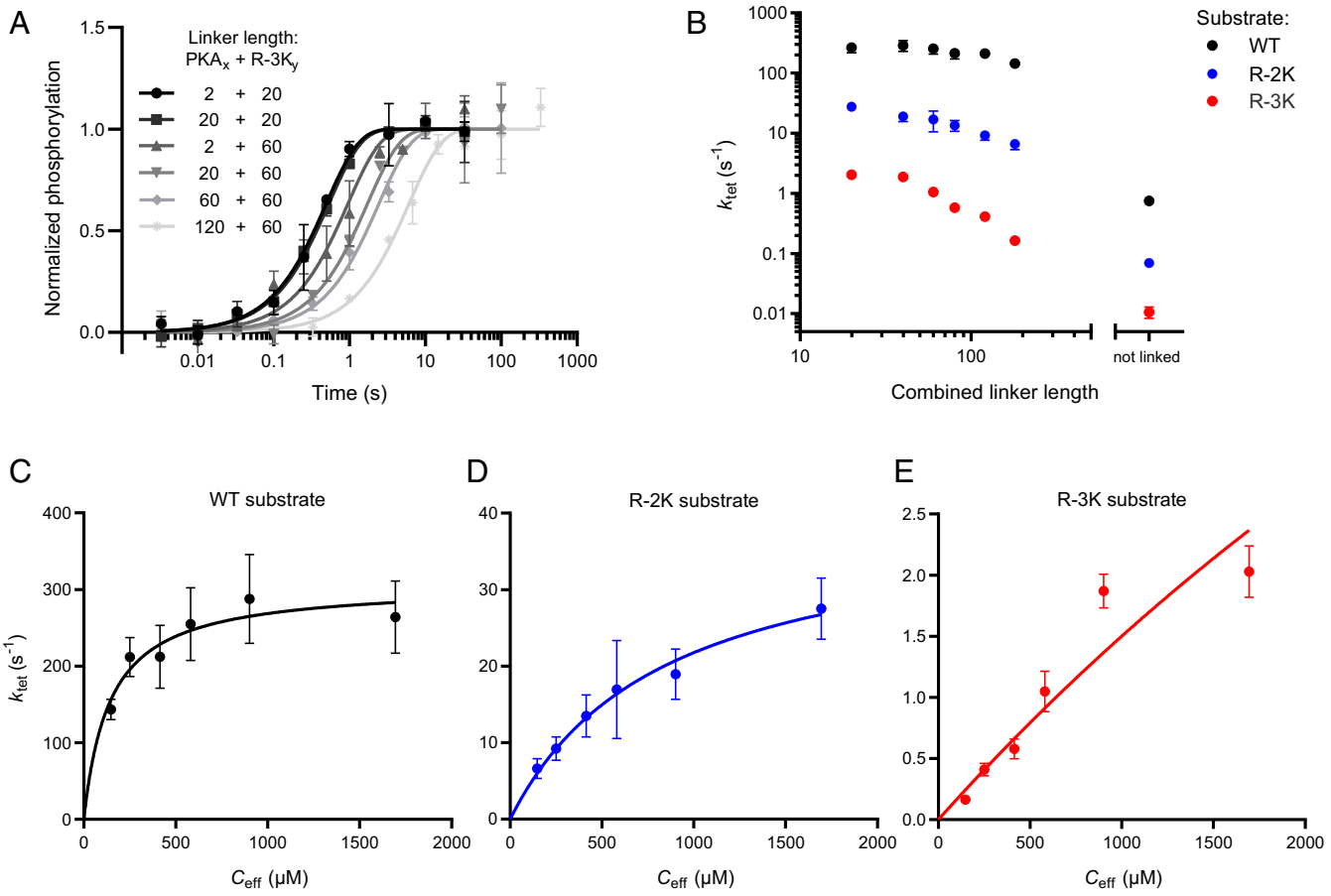

Fig. 2. Linker dependence of single-turnover phosphorylation rates. (*A*) Quench–flow kinetics of the phosphorylation reactions of the R-3K substrate exhibiting the greatest sensitivity to linker length. The total linker length is a combination of contributions from GS repeats in the two constructs labeled PKA_x and $R\text{-}3K_y$, where x and y denote linker length in each construct, listed in the figure. k_{tet} is derived from a fit to one-phase association model (black and gray lines). Error bars indicate mean ± SD, $n = 2$. (*B*) The observed rate of phosphorylation (k_{tet}) of three different substrates as a function of the combined linker length. (*C–E*) Phosphorylation rates as a function of the estimated effective concentration enforced by the linker. Effective concentrations are estimated from the power law measured previously for GS linkers (12) assuming that the presence of the coiled-coil domain is negligible. Error bars correspond to SE of the fit to one-phase association model.

literature value of 200 μM (17), and it increased to 837 and 8,400 μM for R-2K and R-3K, respectively.

To test whether the rates of tethered catalysis can be predicted from steady-state kinetics, we recorded a matching untethered steady-state enzyme kinetics for each substrate (Fig. 4 and *SI Appendix*, Fig. S5). The K_M of the untethered reaction increased from 24.0 μM in the WT substrate to 200 and 973 μM in R-2K and R-3K, respectively. K_M values for all substrates are an order of magnitude below the corresponding K_d values. To quantify the relationship between K_M and K_d, we derived steady-state parameters as a function of rate constants in untethered system (*SI Appendix*, Text), which resulted in the following equation:

$$K_M = K_d \frac{k_3}{k_2 + k_3}. \quad [3]$$

K_M is expected to be smaller than K_d when the steady-state reaction is limited by product dissociation ($k_3 < k_2$). In turn, this

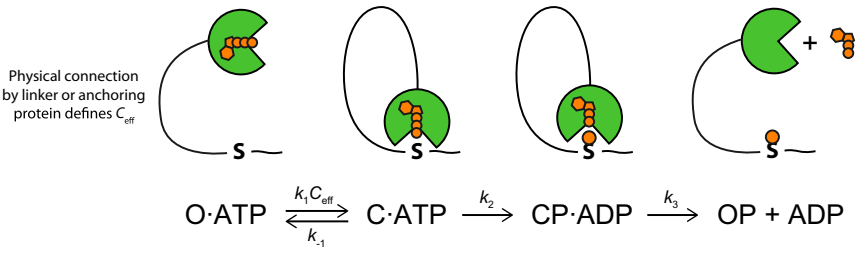

Fig. 3. Generalized kinetic scheme for tethered phosphorylation under saturating concentration of ATP. The kinase (green) is linked to its substrate (S) by a flexible tether that defines C_{eff}. The connection could be a direct fusion via a linker or noncovalent interaction where the lifetime is much longer than the phosphorylation rate. The model consists of a rapid preequilibrium between an open catalytically incompetent state and a closed catalytically competent state (C). Phosphorylation is assumed to be irreversible. Nucleotide and phosphorylation are shown as orange moieties in the cartoon.

Table 1. Kinetic parameters obtained from fits of experimental data to Eq. 1 (tethered) or to Michaelis–Menten model (untethered)

	WT 1 mM ATP	WT	R-2K	R-3K
Tethered				
$k_{tet,max}$ (s^{-1})	415 ± 47	307 ± 21	40.0 ± 3.5	= 14.1
$C_{eff,50}$ (μM)	107 ± 59	142 ± 42	837 ± 150	8,400 ± 910
Untethered				
k_{cat} (s^{-1})		37.3 ± 0.8	33.5 ± 0.4	14.1 ± 0.3
K_M (μM)		24.0 ± 2.1	200 ± 5.2	973 ± 43

Errors correspond to SE of the fit.

suggests tethered and untethered phosphorylation will have different half saturation points as kinases are often limited by product dissociation (25, 26).

The k_{cat} values decreased slightly from 37.3 s^{-1} in WT to 33.5 and 14.1 s^{-1} in R-2K and R-3K, respectively. In contrast, there was a big difference in $k_{tet,max}$ between the substrates: it was eightfold faster than k_{cat} for WT (307 s^{-1}), was roughly the same for R-2K (40.0 s^{-1}), and seemed to be slower (~3 s^{-1}) for R-3K. As $k_{tet,max}$ corresponds to the rate of phosphotransfer, it cannot be lower than k_{cat}. The inconsistency for R-3K is likely due to the poorly defined plateau in the data for tethered R-3K, and thus, we constrained $k_{tet,max}$ to its lower limit equal to k_{cat} upon fitting of the R-3K data. To test how reactions with widely different rates of phosphotransfer can converge on similar steady-state turnover rates, we simulated k_{cat} as a function of $k_{tet,max}$ for different values of the product dissociation rate constant (Fig. 5*A*) as below:

$$k_{cat} = \frac{k_2 k_3}{k_2 + k_3}. \quad [4]$$

Fig. 5*A* shows that k_{cat} is largely independent of the rate of phosphotransfer, when the steady-state reaction is limited by product dissociation. The observed values of k_{cat} can thus roughly be explained assuming the same rate of product dissociation. Product dissociation rates will be similar if ADP dissociation is limiting but may differ for the peptides, so a perfect fit is not expected. Crucially, however, Fig. 5*A* shows that steady-state kinetics only have a limited ability to predict the rate of a tethered reaction, and by extension it cannot predict the relative substrate usage in signaling events that only require a single intracomplex catalytic turnover.

Discussion

We have developed a reductionistic model for phosphorylation by a tethered kinase that mimics key features of kinases that contain disordered linkers or bind flexible scaffolding proteins. The model system omits the complexity of natural signaling complexes but in return allows systematic variation of the linker architecture and substrate. This allowed us to demonstrate that phosphorylation can be enhanced dramatically by tethering, and this enhancement depends strongly on linker length. We used linkers composed solely of GS repeats to approximate a neutral and flexible linker. Natural linkers have diverse sequence compositions, and we anticipate that it will modulate phosphorylation through the effective concentration. The compaction of disordered regions increases with net charge density and rigidity promoting residues such as proline (27, 28). In contrast, ampholytes and patchy charge distribution can cause disordered regions to contract (29). The compaction of the linker determines the volume available to the tethered ligand, and therefore, effective concentrations depend similarly on sequence (12). As tethered phosphorylation depends on effective concentration, it will likely also depend on linker sequence, although this is not directly tested here.

We have shown that single-turnover tethered phosphorylation can be described by a Michaelis–Menten-like dependence on the effective concentration but that the kinetic parameters can only partially be described from steady-state kinetics. The rate of tethered phosphorylation reaches a plateau at high effective concentrations, but is such saturation relevant for kinase reactions in natural signaling complexes? Saturation occurs when the effective substrate concentration exceeds the affinity of the kinase. The affinity of kinases for short substrate motifs can typically reach low μM values, although many biologically important substrates are far from the optimal sequence motif and may have even lower affinities. Model systems and computational modeling suggest that the effective concentrations in protein complexes reach the low mM range (12, 19, 20). This suggests that signaling complexes can reach the saturation regime, where, e.g., the shortening of a linker will no longer enhance the reactions.

Saturation at high effective concentrations provides a mechanism for how changes in the linker architecture can change the relative rate of tethered substrates and thus alter the substrate usage of a kinase. For example, consider two adjacent phosphorylation sites corresponding to the WT and R-3K substrates tethered at the same effective concentration (Fig. 5*B*). If the scaffolding protein changes structure due to, e.g., effector binding or alternative splicing, the effective concentration may change from 100 μM to 1 mM, corresponding to GS-linkers of 257 and 53 residues, respectively. These values roughly match the difference in linkers between the α and β isoforms of CaMKII (30). As the WT substrate is near saturation, the phosphorylation rate of R-3K will be enhanced 4.3-fold more. This suggests that changes in linker architecture that increase effective concentrations shift relative substrate usage toward low-affinity substrates.

Tethered kinases are often part of switch-like functions, where the biological effect only requires phosphorylation of few substrates. Examples include autophosphorylation of kinases such as CaMKII or activation by transphosphorylation of receptor

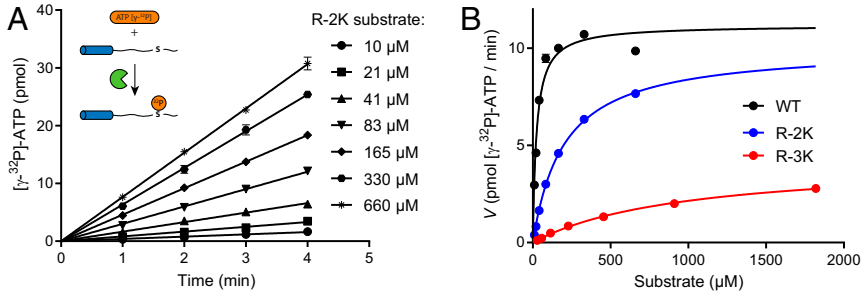

Fig. 4. Quantifying the quality of PKA substrate variants. (*A*) Primary data from a steady-state kinetic experiment performed at 1 nM PKAc and an indicated concentration of the p66α-(QS)-R-2K substrate. Error bars indicate mean ± SD, $n = 3$. (*Inset*) A schematic cartoon of the experiment. (*B*) Steady-state kinetic data of three substrates fitted by a Michaelis–Menten model. Error bars (mostly smaller than the thickness of the round symbols) correspond to SE of the fit to a simple linear regression model.

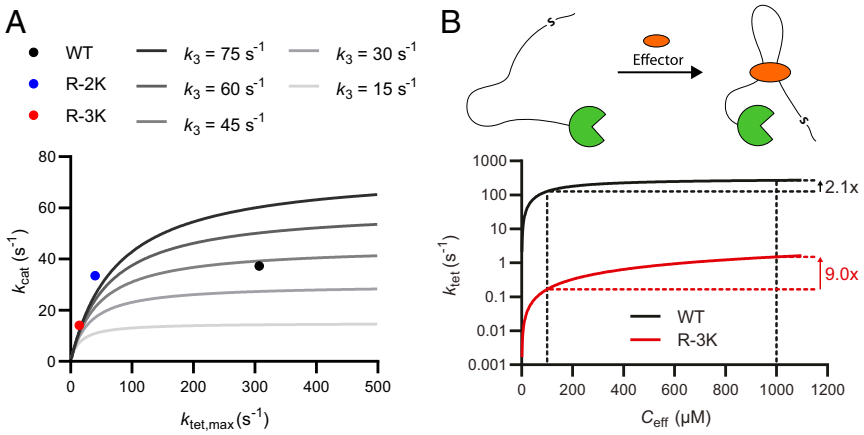

Fig. 5. Simulated predictions for tethered catalysis. (*A*) Simulations of k_{cat} from $k_{tet,max}$ and k_3 based on Eq. 4 in a product release limited reaction. At high $k_{tet,max}$ values, k_{cat} is decoupled from the rate of the tethered reaction and may disguise large differences in the tethered phosphorylation rate. (*B*) Fitting curves from Figs. 2*C* (WT) and 2*E* (R-3K) show unequal increase in k_{tet} (2.1× and 9.0×, respectively) upon increasing C_{eff} from 100 to 1,000 μM.

tyrosine kinases. Furthermore, activatory stimuli are often transient such as, e.g., the brief burst of Ca^{2+} triggered by opening Ca^{2+} channels. In such switches, the number of substrates processed per time is less important than the time required for the first phosphorylation. Yet steady-state kinetics remains the main mode of evaluating substrates, even if the native physiological context is a tethered complex. We show that steady-state parameters can disguise big differences in the rate of tethered phosphorylation: The WT and R-2K substrates had an eightfold difference in $k_{tet,max}$ even though the k_{cat} values are similar. This occurs because product dissociation limits the steady-state reaction but not the phosphorylation of tethered substrate. The latter is more relevant to tethered kinases with switch-like functions, which suggests that substrate properties should be evaluated in single-turnover experiments.

Kinases are often tethered to substrates via noncovalent interactions, which suggests that dissociation and rebinding should be considered. The model proposed here only considers a static connection, even though the fitted data use a noncovalent connection between kinase and substrate. We suggest that the interaction can be approximated as static, when its lifetime is much longer than the catalytic cycle. As such our model system describes high-affinity scaffolding interactions in addition to linkers that are truly static, such as in kinase autophosphorylation reactions. For weaker interactions, single-turnover and steady-state kinetic models start to blend and will accordingly be more complex. We believe that the static model will provide a baseline for such efforts.

During the preparation of this manuscript, a manuscript appeared with similar aims but very different results (31). In agreement with our results, Speltz and Zalatan (31) found that for tethered PKAc, shorter linkers increased the rate of phosphorylation, although the linker dependence was not monotonic for longer linkers. Despite the similarity between the model systems used, the reaction occurred in a different kinetic regime with a maximal k_{tet} of ~0.002 s^{-1}. The unexpectedly slow phosphorylation rate was explained by effective concentrations of ~80 nM, which is 50,000-fold below prediction from a simple geometric model (31). The systems differ mainly in the linkers, as Speltz and Zalatan (31) use linkers that also contain a folded domain. Likely, the discrepancy between experimental and predicted values shows the limitation of simple polymer models for short linkers with embedded folded domains. Such systems can easily become sterically limited by the excluded volume from folded domains and sequence-specific interactions that lead to internal friction. In contrast, long disordered linkers allow almost free orientation of domains (32) and are likely to provide the most robust architecture for engineered scaffolding proteins.

Tethered reactions are not just important for kinases. Tethering is arguably even more important for phosphatases as the substrate motif contributes little specificity. Instead, phosphatases are regulated by anchoring proteins, and, e.g., protein phosphatase-1 has at least 200 different regulatory subunits that target it to different substrates (33). These anchoring interactions likely display a similar dependence for linker architecture as seen here. Tethering is also increasingly used as a therapeutic intervention strategy. Enzymes tethering is important in, e.g., PROTACs that target proteins for degradation by tethering them to ubiquitin ligase (34). Tethering has also been used pharmacologically to enhance other classes of enzymes including, e.g., proteases (35) and phosphatases (36). Such connector molecules will likely display a similar dependence on connection to the systems studied here, and mechanistic studies of tethered catalysis are thus of fundamental importance both to understand signaling pathways and to optimize pharmaceutical intervention strategies.

Data Availability. All relevant data are included in the manuscript and *SI Appendix*.

ACKNOWLEDGMENTS. This work was supported by grants to M.K. from the Young Investigator Program of the Villum Foundation, the Aarhus Institute of Advanced Studies COFUND program funded by the Seventh Framework Programme of the European Union (Agreement 754513), and Center for Proteins in Memory, a Center of Excellence funded by the Danish National Research Foundation (Grant DNRF133).

1. K. Taskén, E. M. Aandahl, Localized effects of cAMP mediated by distinct routes of protein kinase A. *Physiol. Rev.* **84**, 137–167 (2004).
2. C. J. Miller, B. E. Turk, Homing in: Mechanisms of substrate targeting by protein kinases. *Trends Biochem. Sci.* **43**, 380–394 (2018).
3. T. Pawson, Protein modules and signalling networks. *Nature* **373**, 573–580 (1995).
4. M. C. Good, J. G. Zalatan, W. A. Lim, Scaffold proteins: Hubs for controlling the flow of cellular information. *Science* **332**, 680–686 (2011).
5. W. Wong, J. D. Scott, AKAP signalling complexes: Focal points in space and time. *Nat. Rev. Mol. Cell Biol.* **5**, 959–970 (2004).
6. F. D. Smith *et al.*, Local protein kinase A action proceeds through intact holoenzymes. *Science* **356**, 1288–1293 (2017).
7. F. D. Smith *et al.*, Intrinsic disorder within an AKAP-protein kinase A complex guides local substrate phosphorylation. *eLife* **2**, e01319 (2013).
8. M. Bhattacharyya *et al.*, Flexible linkers in CaMKII control the balance between activating and inhibitory autophosphorylation. *eLife* **9**, e53670 (2020).
9. S. S. Taylor, R. Ilouz, P. Zhang, A. P. Kornev, Assembly of allosteric macromolecular switches: Lessons from PKA. *Nat. Rev. Mol. Cell Biol.* **13**, 646–658 (2012).
10. A. L. Bauman *et al.*, Dynamic regulation of cAMP synthesis through anchored PKA-adenylyl cyclase V/VI complexes. *Mol. Cell* **23**, 925–931 (2006).
11. M. S. Cortese, V. N. Uversky, A. K. Dunker, Intrinsic disorder in scaffold proteins: Getting more from less. *Prog. Biophys. Mol. Biol.* **98**, 85–106 (2008).

12. C. S. Sørensen, M. Kjaergaard, Effective concentrations enforced by intrinsically disordered linkers are governed by polymer physics. *Proc. Natl. Acad. Sci. U.S.A.* **116**, 23124–23131 (2019).
13. N. Narayana, S. Cox, S. Shaltiel, S. S. Taylor, N. Xuong, Crystal structure of a polyhistidine-tagged recombinant catalytic subunit of cAMP-dependent protein kinase complexed with the peptide inhibitor PKI(5-24) and adenosine. *Biochemistry* **36**, 4438–4448 (1997).
14. F. W. Studier, Protein production by auto-induction in high density shaking cultures. *Protein Expr. Purif.* **41**, 207–234 (2005).
15. B. E. Kemp, D. J. Graves, E. Benjamini, E. G. Krebs, Role of multiple basic residues in determining the substrate specificity of cyclic AMP-dependent protein kinase. *J. Biol. Chem.* **252**, 4888–4894 (1977).
16. M. N. Gnanapragasam *et al*., p66Alpha-MBD2 coiled-coil interaction and recruitment of Mi-2 are critical for globin gene silencing by the MBD2-NuRD complex. *Proc. Natl. Acad. Sci. U.S.A.* **108**, 7487–7492 (2011).
17. B. D. Grant, J. A. Adams, Pre-steady-state kinetic analysis of cAMP-dependent protein kinase using rapid quench flow techniques. *Biochemistry* **35**, 2022–2029 (1996).
18. D. Van Valen, M. Haataja, R. Phillips, Biochemistry on a leash: The roles of tether length and geometry in signal integration proteins. *Biophys. J.* **96**, 1275–1292 (2009).
19. C. S. Sørensen, A. Jendroszek, M. Kjaergaard, Linker dependence of avidity in multivalent interactions between disordered proteins. *J. Mol. Biol.* **431**, 4784–4795 (2019).
20. E. T. Mack *et al*., Dependence of avidity on linker length for a bivalent ligand-bivalent receptor model system. *J. Am. Chem. Soc.* **134**, 333–345 (2012).
21. D. J. Diestler, E. W. Knapp, Statistical thermodynamics of the stability of multivalent ligand-receptor complexes. *Phys. Rev. Lett.* **100**, 178101 (2008).
22. W. Borcherds *et al*., Optimal affinity enhancement by a conserved flexible linker controls p53 mimicry in MdmX. *Biophys. J.* **112**, 2038–2042 (2017).
23. K. P. Sherry, R. K. Das, R. V. Pappu, D. Barrick, Control of transcriptional activity by design of charge patterning in the intrinsically disordered RAM region of the Notch receptor. *Proc. Natl. Acad. Sci. U.S.A.* **114**, E9243–E9252 (2017).
24. J. A. Adams, Kinetic and catalytic mechanisms of protein kinases. *Chem. Rev.* **101**, 2271–2290 (2001).
25. P. F. Cook, M. E. Neville Jr., K. E. Vrana, F. T. Hartl, R. Roskoski Jr., Adenosine cyclic 3′,5′-monophosphate dependent protein kinase: Kinetic mechanism for the bovine skeletal muscle catalytic subunit. *Biochemistry* **21**, 5794–5799 (1982).
26. S. Whitehouse, D. A. Walsh, Mg X ATP2-dependent interaction of the inhibitor protein of the cAMP-dependent protein kinase with the catalytic subunit. *J. Biol. Chem.* **258**, 3682–3692 (1983).
27. J. A. Marsh, J. D. Forman-Kay, Sequence determinants of compaction in intrinsically disordered proteins. *Biophys. J.* **98**, 2383–2390 (2010).
28. A. H. Mao, S. L. Crick, A. Vitalis, C. L. Chicoine, R. V. Pappu, Net charge per residue modulates conformational ensembles of intrinsically disordered proteins. *Proc. Natl. Acad. Sci. U.S.A.* **107**, 8183–8188 (2010).
29. R. K. Das, R. V. Pappu, Conformations of intrinsically disordered proteins are influenced by linear sequence distributions of oppositely charged residues. *Proc. Natl. Acad. Sci. U.S.A.* **110**, 13392–13397 (2013).
30. R. Sloutsky *et al*., Heterogeneity in human hippocampal CaMKII transcripts reveals allosteric hub-dependent regulation. *Sci. Signal* **13**, 10.1126/scisignal.aaz0240 (2020).
31. E. B. Speltz, J. G. Zalatan, The relationship between effective molarity and affinity governs rate enhancements in tethered kinase-substrate reactions. *Biochemistry* **59**, 2182–2193 (2020).
32. A. Mittal, A. S. Holehouse, M. C. Cohan, R. V. Pappu, Sequence-to-conformation relationships of disordered regions tethered to folded domains of proteins. *J. Mol. Biol.* **430**, 2403–2421 (2018).
33. M. Bollen, W. Peti, M. J. Ragusa, M. Beullens, The extended PP1 toolkit: Designed to create specificity. *Trends Biochem. Sci.* **35**, 450–458 (2010).
34. S. L. Paiva, C. M. Crews, Targeted protein degradation: Elements of PROTAC design. *Curr. Opin. Chem. Biol.* **50**, 111–119 (2019).
35. T. Kitazawa *et al*., A bispecific antibody to factors IXa and X restores factor VIII hemostatic activity in a hemophilia A model. *Nat. Med.* **18**, 1570–1574 (2012).
36. S. Yamazoe *et al*., Heterobifunctional molecules induce dephosphorylation of kinases—A proof of concept study. *J. Med. Chem.* **63**, 2807–2813 (2020).